NJOY Maximum Energy Limit For Thermal Neutron Cross Section Treatment

Yunhuang Zhang, Aaron J. Holzaepfel, Marvin L. Adams

Department of Nuclear Engineering, Texas A&M University, College Station, TX 77843
yunhuangz@tamu.edu, aholzaepfel@email.tamu.edu, mladams@tamu.edu

Abstract - *This paper explores the proper choice of upper energy cut-off (emax) for thermal treatment in NJOY when NJOY is used to generate multigroup cross sections. We suggest that in some problems it is important to use a value of emax that is well above NJOY2012's internal limit of 10 eV. A patch provided by Los Alamos National Laboratory (LANL) raises the emax limit to 100 eV, which greatly improved the accuracy of our multi-group simulation results in problems containing hydrogen and a strong thermal absorber.*

I. INTRODUCTION

When thermal motion of target nuclei and/or binding of the target atoms in molecules or lattices significantly affects the neutron scattering cross sections, the effects cannot be ignored in high-fidelity calculations. In NJOY, a dedicated module, THERMR[1], is responsible for processing the thermal scattering cross sections. One of the user-defined parameters in THERMR is the thermal cut-off energy (*emax*), which specifies the maximum neutron incident energy to which THERMR will apply thermal treatment. Since the thermal and epithermal neutrons tend to carry speeds comparable with target nuclei and energy comparable to target molecules binding energies, it is not uncommon to see *emax* set to a value between 0.1 eV and 10 eV. In fact, as found in NJOY2012, THERMR has a hard-coded *emax* upper limit of 10 eV. However, our studies suggest that in problems with a hydrogenous scatterer and a thermal-neutron absorber, a higher *emax* is needed to obtain accurate results. Raising this limit requires modifying the NJOY source code, at least in the versions we have used in our work (including NJOY212).

II. HYDROGEN SCATTERING CROSS SECTION ANALYSIS

Hydrogen is the main scatterer in our the borated high-density polyethylene (B-HDPE) test problem that we use for illustration in this paper. It is also the simplest target nucleus, whose non-thermal (target nucleus at rest) neutron scattering analytic form can be derived with classic two-body kinematics, as well as one of the most important neutron moderating material in modern reactor applications. In order to understand the thermal treatment effect on scattering cross sections and the proper choice of *emax*, we studied the secondary energy distribution of the elastic scattering of Hydrogen.

1. Analytic Secondary Energy Distribution for Non-thermal Scattering

Recall that when neutrons scatter off a Hydrogen nucleus at rest, the scattering angle distribution in the center-of-mass reference frame is isotropic. Therefore, according to two-body kinematics, the secondary distribution of the post-scatter neutrons is uniform between 0 eV and its incident energy, and zero elsewhere[2]. That is, the secondary energy distribution,

$P_E(E \rightarrow E')$, can be expressed as follows:

$$P_E(E \rightarrow E') = \begin{cases} 0, & E' > E \\ \frac{1}{E}, & 0 \le E' \le E \end{cases} \qquad (1)$$

where E is neutron incident energy, and E' is neutron outgoing energy.

2. Thermal Scattering Secondary Energy Distribution: Multi-group vs. MCNP Comparison

With the analytic non-thermal secondary energy distribution in mind, we compared the thermal secondary energy distributions given by NJOY-generated multi-group transfer cross sections against the ones generated by MCNP using continuous energy ACE cross section data, for both cases of free-gas and $S(\alpha, \beta)$ thermal treatment[1]. We used MCNP as reference because it uses its own kinematics model for computing free-gas thermal corrections. Therefore, MCNP's free-gas behavior is totally independent of NJOY's thermal treatment procedure and thus is not subject to the *emax* limit, even if the ACE file is originally generated by NJOY. For $S(\alpha, \beta)$ treatment, MCNP uses the $S(\alpha, \beta)$ data in the ACE file whenever available, and uses its own free-gas treatment when incident neutron energy goes beyond $S(\alpha, \beta)$ data table's range.

The MATXS format was chosen as the format for the multi-group cross section. The MATXS file was generated using NJOY2012 with ENDF/B-VII.1 library and *emax*=100 eV. The discrete secondary energy distributions for each incident energy group can be extracted by taking the columns of the elastic scattering transfer matrix (assuming column indices correspond to incident neutron energies and row indices to secondary (scattered) neutron energies). On the continuous-energy side, a group-to-group transfer matrix is not readily available from the ACE file due to its continuous energy nature. To infer the correct multi-group secondary energy distribution information from the continuous-energy data, we designed and ran a thin wire problem in MCNP. The wire is composed of Hydrogen as the target medium and is extremely thin (10^{-12} mean free paths (mfp) in cross-sectional diameter) and long (10^6 mfp in length). A mono-energetic uni-directional neutron source is incident along the axis of the wire, and neutrons passing through the wire surface as a result of scattering with Hydrogen were tallied. As the wire's diameter approaches zero, any neutron that changes its flight direction (therefore its energy) during a scattering event will exit and be tallied. The

tally is binned in energy using the same group structure that we used when generating the MATXS file with NJOY. This tally renders us a discrete, multi-group-like like energy spectrum for the first-collided scattering source, which is proportional to the secondary energy distribution for a given incident neutron energy:

$$P_E(E \rightarrow E') \propto \Sigma_s(E \rightarrow E')\Phi^{(0)}(E) = \lim_{\substack{R \rightarrow 0 \\ L \rightarrow \infty}} \oiint J(E')dA \quad (2)$$

where $\Phi^{(0)}(E)$ is the uncollided flux and $J(E')$ is the neutron current through the wire surface. One such MCNP simulation yields the secondary energy distribution for incident neutrons bearing the given incident-neutron energy.
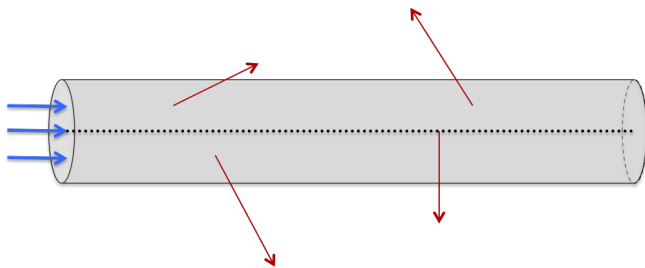
Fig. 1. Thin-wire simulation illustration [not drawn to scale]

By repeating the MCNP simulation for various source energies corresponding to energy group mid-points, we obtained the discrete secondary energy distributions for various discrete incident energies, which are then compared with the same distributions extracted from the elastic scattering transfer matrix found in the MATXS file. To eliminate source of errors in raw cross section data, the ACE files used in MCNP simulation were generated using the same NJOY2012 code and ENDF/B-VII.1 library, with the same *emax* setting. The free-gas secondary energy distribution for selected incident neutron energies is shown in Fig. 2.

It can be seen from Fig. 2 that although we set *emax*=100 eV, NJOY free-gas thermal treatment for multi-group cross sections is restricted to incident neutron energy below 10 eV. For incident neutron energy greater than 10 eV, the scattering cross section reverts back to its non-thermal form prescribed by the Eq. (1). This is a hard-coded internal limit that is not described in the NJOY2012 manual. On the other hand, MCNP applies free-gas treatment all the way to the highest incident energy. Also, in the multi-group results, there are also some low-end tail anomalies observed for incident energies above several hundreds of eV. These can be attributed to the lack of numerical precision in the GROUPR module of NJOY, according to our correspondence with NJOY team at Los Alamos National Laboratory (LANL). The impact of this numerical error on the B-HDPE slowing-down spectrum is negligible.

A second case is the HDPE secondary energy distribution including $S(\alpha, \beta)$ treatment of molecular binding effects, where we examined Hydrogen's binding effect in polyethylene (H-poly). The secondary energy distribution for this case is given in Fig. 3.

Similar to the free-gas Hydrogen case, NJOY only applies $S(\alpha, \beta)$ thermal treatment for incident energies below 10 eV,
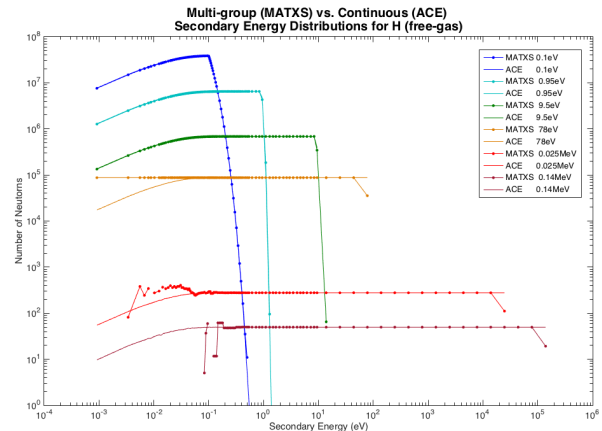
Fig. 2. Hydrogen scattering secondary energy distribution: ACE vs. MATXS (free-gas), *emax* set to 100 eV, original NJOY2012 version. A pair of curves is shown for each of six pre-scatter neutron energies. Each pair of curves shows the scattered-neutron energy distribution from the MCNP thin-wire test problem (continuous-energy cross-sections with MCNP kinematics) and from the NJOY2012-generated multi-group cross sections. Multigroup errors are evident for pre-scatter neutron energies above 10 eV, because the original NJOY has an internal hard-coded cutoff of 10 eV for thermal treatment.

while MCNP applies thermal treatment for the whole incident energy range, despite the fact that the ACE thermal cross section files it uses were also generated by NJOY2012 with the same settings. As will be shown in Section 3., MCNP actually uses the $S(\alpha, \beta)$ data when it is available, in our case, that is for incident energy less than 10 eV. For incident energies above that limit, MCNP uses its own free-gas physics model to correct for thermal cross sections. This behavior should have been expected because MCNP handles free-gas treatment and $S(\alpha, \beta)$ treatment separately: TMP card for free-gas and MT card for $S(\alpha, \beta)$. It is a different approach from NJOY's multi-group cross section processing in that NJOY encompasses all the thermal information into a single thermal scattering matrix. We found MCNP's approach to be more robust, and more realistic as well. Because when incident neutron energy is high enough to overcome the binding energy of the target nuclei in its molecule structure, the neutron will interact with the target nuclei more like a free target. Or in the crystalline lattice sense, the higher the neutron energy, the shorter the neutron's wave length, hence the less effect of neutron diffraction. However, it is still important to find out the proper *emax* for $S(\alpha, \beta)$ treatment so that the binding effect can be fully accounted for. At least in the case of Hydrogen bonded in polyethylene, the trend in Fig. 3 shows that binding effect does not die out at 100 eV.
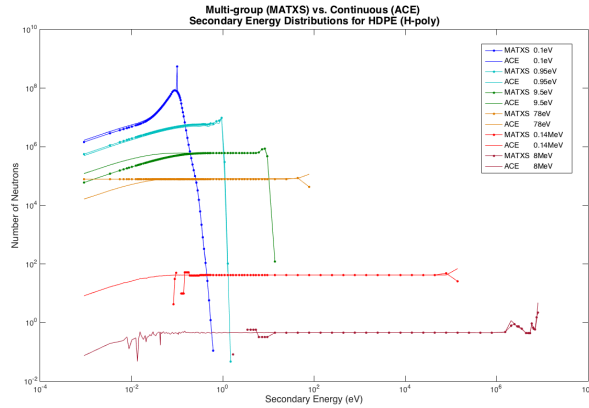
Fig. 3. Hydrogen scattering secondary energy distribution: ACE vs. MATXS (H-poly), *emax* set to 100 eV, original NJOY2012 version. As in the previous figure, but with binding effects taken into account for the H bound in polyethylene.

Fig. 4. Hydrogen scattering secondary energy distribution: ACE vs. MATXS (free-gas), *emax*=100 eV with patch

3. Thermal Scattering Secondary Energy Distribution: Multi-group vs. MCNP Comparison (with Patch)

In recognition of the insufficient thermal treatment energy limit in the THERMR module, we requested and LANL delivered a patch to raise the *emax* limit to 100 eV. We repeated the secondary energy distribution analyses presented the Section 2. upon applying the patch. Fig. 4 and Fig. 5 confirm that both free-gas and $S(\alpha,\beta)$ thermal treatment can now be applied to incident energy up to 100 eV with the patch and the trend of thermal effects continues as expected. However, when running MCNP with updated HDPE cross sections we encountered another problem. That is, although NJOY can apply $S(\alpha,\beta)$ treatment up to 100 eV for the ACE files, MCNP will fail with a segmentation fault when running the same thin-wire problem with the ACE files generated with *emax*>20 eV. Reducing the number of particles alleviates the problem but it incurs higher statistical noise. It appears to be a memory issue but the size of the ACE file was only increased by 10%. It indicates that there might be some compatibility issue between MCNP and the temporary NJOY patch, or it might be that the $S(\alpha,\beta)$ table itself needs to be regenerated with NJOY's LEAPR module to accommodate for increased *emax*. This remains to be investigated.

For the reason stated above, in Fig. 5 the $S(\alpha,\beta)$ thermal treatment for ACE file was only done to incident energies below 20 eV. This leads to an interesting case for E=78 eV, in which the multi-group cross section receives full $S(\alpha,\beta)$ treatment, while the ACE cross sections gets no $S(\alpha,\beta)$ treatment thus only free-gas correction was applied by MCNP itself. Fig. 6 shows multi-group and MCNP produced secondary energy distributions for this case, together with another ACE secondary energy distribution with free-gas treatment as a reference.

It can be seen from Fig. 6 that "ACE 78eV $S(\alpha,\beta)$" results are identical to those of "ACE 78eV Free-gas." This demonstrates that MCNP applies free-gas treatment in the absence of $S(\alpha,\beta)$ data. Fig. 6 also tells us that in the case of H-poly, the $S(\alpha,\beta)$ scattering cross section allows less neutron
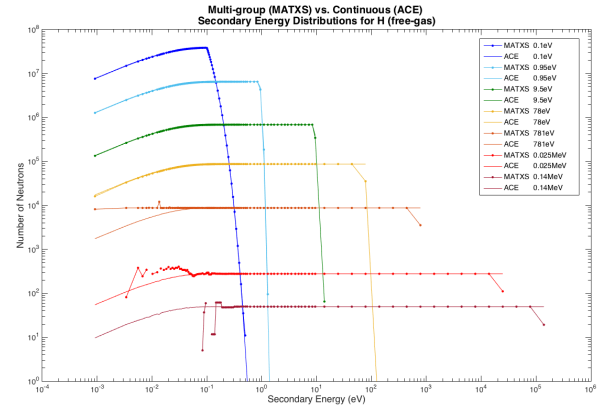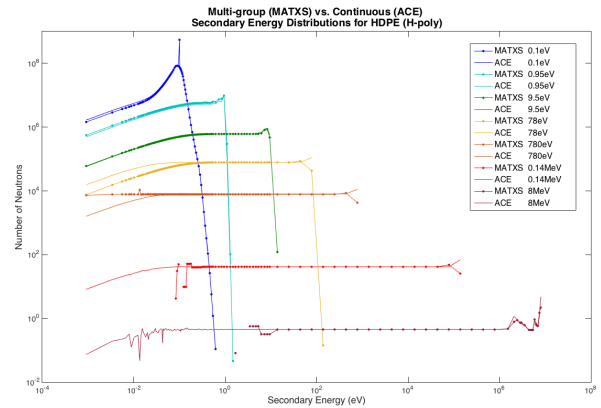
Fig. 5. Hydrogen scattering secondary energy distribution: ACE vs. MATXS (H-poly), *emax*=100 eV with patch

down-scattered into the lowest energy range when compared to the free-gas counterpart. This observation helps us better understand the B-HDPE test problem results to be presented in the next section.

III. B-HDPE RESULT WITH INCREASING THERMAL CUT-OFF

We computed the neutron spectrum in an infinite medium of B-HDPE with an AmBe distributed neutron source, using in-house Parallel Deterministic Transport code (PDT), and compared the results against MCNP simulation results. We used MATXS multi-group cross section for PDT and ACE continuous energy cross sections for MCNP, both generated by NJOY2012 using ENDF/B-VII.1 library. Initially, we ran two PDT cases: One with MATXS cross sections generated with *emax* set to 1 eV and the other with *emax* set to 10 eV. Later, a third case was run with *emax* set to 100 eV, thanks to the patch. MCNP simulation was run with ACE cross sections generated with *emax*=20 eV because of the compatibility problem mentioned previously.

It can be seen from Fig. 7 that in the medium to high
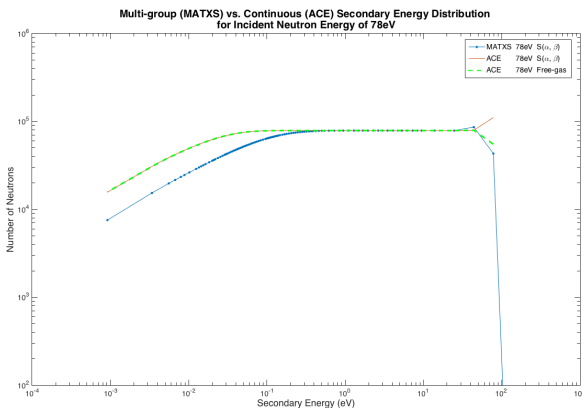
Fig. 6. Hydrogen scattering secondary energy distribution: ACE vs. MATXS, *E*=78 eV, ***emax***=100 eV with patch
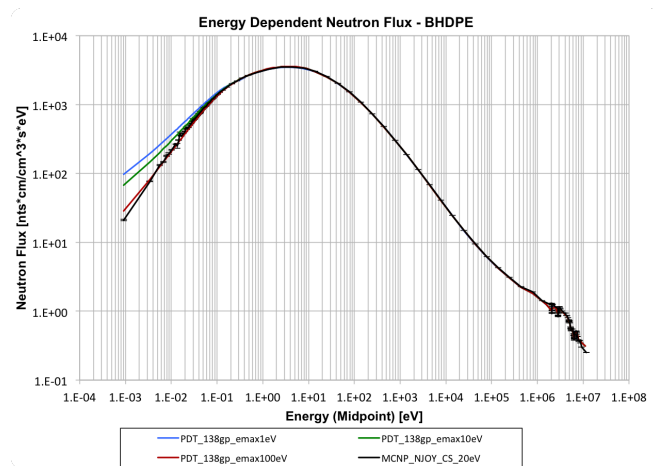
Fig. 7. Neutron spectrum in infinite B-HDPE with AmBe distributed source. The curve that is lowest in the low-energy range is the continuous-energy MCNP result. The three multi-group results with ***emax*** = 1 eV, 10 eV, and 100 eV approach the continuous-energy result as ***emax*** increases.

energy range, PDT results match MCNP results quite well. In the lower energy end of the spectrum, as we increase *emax* successively from 1 eV to 10 eV and then to 100 eV, the PDT multigroup solutions yields consistently better agreement with MCNP.

However, even with ***emax***=100 eV, PDT's solution at the low energy end is still slightly higher than MCNP's solution. That is because multi-group cross sections do not receive any thermal treatment for incident energy above the thermal cutoff while MCNP applies free-gas treatment across the entire incident energy range even when $S(\alpha, \beta)$ data is not available. That means PDT over-predicts the number of neutrons slowed down to the very low energy region as compared to MCNP, which itself over-predicts the solution in the same energy range relative to physical truth because the free-gas model tends to produce a higher secondary energy distribution in the low energy end when compared to $S(\alpha, \beta)$ model, as shown in

Fig. 6. Another discrepancy is not as prominent and can be only seen in the zoomed-in plot shown in Fig. 8. It shows that MCNP solution is ever slightly higher than PDT solution in the energy range between 0.01 eV and 0.1 eV. The reason can be attributed mostly to the fact that MCNP uses free-gas treatment (no binding) whenever $S(\alpha, \beta)$ data is not available from the ACE file. In these calculations, for incident energy between 20 eV and 100 eV, the multi-group cross sections included $S(\alpha, \beta)$ treatment of binding effects, whereas MCNP was forced to use its own free-gas treatment (no binding). Our experience and analysis suggest that with an MCNP-compatible NJOY patch, which would allow us to use higher thermal cut-offs for both multi-group and ACE cross sections, accurately treating both thermal motion and binding effects, a better agreement between continuous-energy (MCNP) and multi-group (PDT, for example) could be achieved.
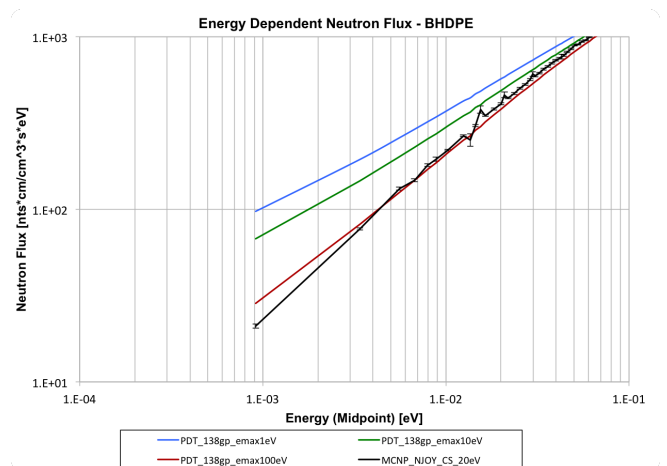
Fig. 8. Neutron spectrum in infinite B-HDPE with AmBe distributed source [Zoom-in]

It is worth pointing out that the phenomena described here was observed only in a hydrogenous scatterer with a strong thermal absorber (in our case HDPE with Boron). Without hydrogen, neutrons cannot directly scatter from above the thermal range to the lower portions of the thermal range. If there is no thermal absorber, then the scattering (both down-scatter and up-scatter) of thermal neutrons will dominate and force a Maxwellian-shaped spectrum as dictated by statistical mechanics.

IV. CONCLUSIONS

In this work we have demonstrated that although it seems plausible to set NJOY THERMR ***emax*** to a value in the 0.1 eV to 10 eV range, for problems with hydrogen and a strong thermal absorber and a fast or epithermal neutron source, a higher thermal cut-off is desirable for higher fidelity of the simulation results. A temporary NJOY2012 patch from LANL allowed us to demonstrate positive improvements in results from a thermal cutoff that was much higher than the internal limit in the original NJOY2012 code.

V. ACKNOWLEDGMENTS

REFERENCES

1. R. E. MACFARLANE, "The NJOY Nuclear Data Processing System, Version 2012," Tech. Rep. LA-UR-12-27079, Los Alamos National Laboratory (2013).
2. J. R. LAMARSH and A. J. BARATTA, *Introduction to Nuclear Engineering*, Pearson, 3rd ed. (2001).